Author Manuscript

Author Manuscript

Author Manuscript

Author Manuscript

HHS Public Access

Author manuscript

Cell Rep. Author manuscript; available in PMC 2018 January 24.

Published in final edited form as:

Cell Rep. 2017 January 24; 18(4): 831–839. doi:10.1016/j.celrep.2016.12.074.

Germ cell-less promotes centrosome segregation to induce germ cell formation

Dorothy A. Lerit[1,7,8], **Conrad W. Shebelut**[2], **Kristen J. Lawlor**[3], **Nasser M. Rusan**[4], **Elizabeth R. Gavis**[5], **Paul Schedl**[5,6], and **Girish Deshpande**[5,7]

[1]Department of Cell Biology, Emory University School of Medicine, Atlanta, GA 30322

[2]School of Medicine, University of Virginia, Charlottesville, VA 22908

[3]Department of Neuroscience, Columbia University, New York, NY 10032

[4]Cell Biology and Physiology Center; National Heart, Lung, and Blood Institute; National Institutes of Health; Bethesda, MD 20892

[5]Department of Molecular Biology, Princeton University, Princeton, NJ 08544

[6]Laboratory of Gene Expression Regulation in Development, Institute of Gene Biology, Russian Academy of Sciences, Moscow, Russia 119991

Abstract

The primordial germ cells (PGCs) specified during embryogenesis serve as progenitors to the adult germline stem cells. In *Drosophila*, the proper specification and formation of PGCs requires both centrosomes and germ plasm, which contains the germline determinants. Centrosomes are microtubule (MT)-organizing centers that ensure the faithful segregation of germ plasm into PGCs. To date, mechanisms that modulate centrosome behavior to engineer PGC development have remained elusive. Only one germ plasm component, Germ cell-less (Gcl), is known to play a role in PGC formation. Here, we show that Gcl engineers PGC formation by regulating centrosome dynamics. Loss of *gcl* leads to aberrant centrosome separation and elaboration of the astral MT network, resulting in inefficient germ plasm segregation and aborted PGC cellularization. Importantly, compromising centrosome separation alone is sufficient to mimic the *gcl* loss-of-function phenotypes. We conclude Gcl functions as a key regulator of centrosome separation required for proper PGC development.

Contact Information: Dorothy A. Lerit (Lead Contact), Department of Cell Biology, Emory University School of Medicine, Atlanta, GA 30322, dlerit@emory.edu, Girish Deshpande, Department of Molecular Biology, Princeton University, Princeton, NJ 08544, gdeshpan@princeton.edu.

[7]Co-corresponding Authors

[8]Lead Contact

Author Contributions

Conceptualization and Methodology, DAL and GD; Formal Analysis, DAL, CWS, GD; Investigation, DAL, KL, GD; Writing-Original Draft, DAL and GD; Writing-Review & Editing, DAL, CWS, NMR, ERG, PS, and GD; Funding Acquisition, DAL, NMR, ERG, PS, and GD.

Publisher's Disclaimer: This is a PDF file of an unedited manuscript that has been accepted for publication. As a service to our customers we are providing this early version of the manuscript. The manuscript will undergo copyediting, typesetting, and review of the resulting proof before it is published in its final form. Please note that during the production process errors may be discovered which could affect the content, and all legal disclaimers that apply to the journal pertain.

Author Manuscript Author Manuscript Author Manuscript Author Manuscript

eTOC Blurb

Primordial germ cells (PGCs) are the totipotent progenitors for the next generation. Lerit, et al. show proper PGC development requires Germ cell-less to instruct the spatial distribution of centrosomes within syncytial *Drosophila* embryos and ensure the efficient segregation of the germline fate determinants.

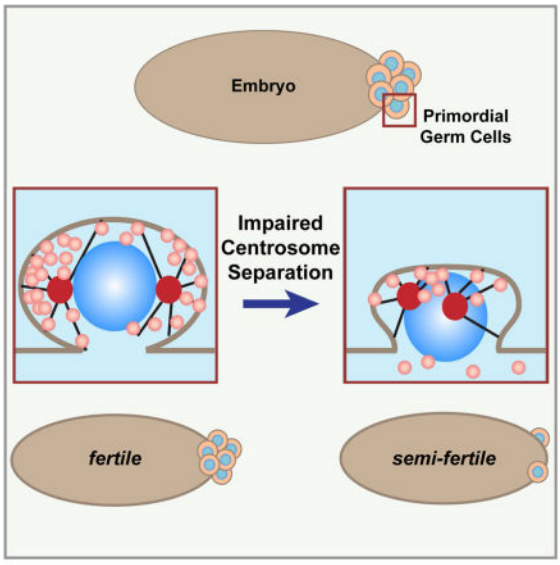

Keywords

cell fate; germ cells; centrosome; germ plasm; germ cell-less; stem cells

Introduction

Primordial germ cells (PGCs) serve as precursors to the adult germline stem cells (GSCs) and are set aside early in embryogenesis (Ewen-Campen et al., 2010). In syncytial *Drosophila* embryos, for example, somatic nuclei undergo a series of rapid, synchronous nuclear divisions before cellularization at the end of nuclear cycle (NC) 14 (Foe and Alberts, 1983). In contrast, PGCs are formed at the posterior pole of the early embryo during NC 10. The precocious cellularization of PGCs depends upon maternally derived germline determinants, called the germ plasm, which is analogous to mammalian nuage. Components of the germ plasm localize to the posterior actin cortex during oogenesis, where they remain throughout early embryogenesis (Mahowald, 2001). PGC formation is characterized by the actin-dependent protrusion of pole buds (PBs) from the posterior embryonic cortex followed by the closure of actin-rich contractile rings, or PB furrows, at the base of each PB (Warn et al., 1985).

Because budding coincides with the migration of several nuclei into the posterior region of the embryo, nuclear proximity to the posterior pole was initially thought to trigger PB formation. This model was directly tested by pharmacological studies in which aphidicolin was injected into NC 7–8 embryos to inhibit DNA synthesis and impair nuclear migration

Author Manuscript Author Manuscript Author Manuscript Author Manuscript

(Raff and Glover, 1989). Importantly, despite the inability of nuclei to reach the posterior cortex, PGCs formed at the posterior pole in drug-treated embryos. Furthermore, restructuring of the actin cytoskeleton to promote PGC formation could be attributed to the coordinated migration of centrosomes that had uncoupled from the accompanying nuclei and reached the posterior pole (Raff and Glover, 1989, Raff et al., 1990). Thus, the anucleated centrosomes and their associated astral microtubules (MTs) were sufficient to initiate the process of PGC formation.

The role of the centrosomes in germline development was revisited using live imaging of the germ plasm components *nanos* (*nos*; Smith et al., 1992) RNA and Vasa (Vas; Lasko and Ashburner, 1990) protein. This work demonstrated that centrosomes and their associated MTs promote the release of cortically anchored germ plasm and its subsequent dynein-dependent transport and accumulation around PB nuclei (Lerit and Gavis, 2011). This active transport program ensures the passage of the germline determinants into the PGCs.

Among the different components involved in PGC determination, Germ cell-less (Gcl; Jongens et al., 1992) is of special interest because it is the only one known to be involved not only in PGC specification but also in the actual formation of PGCs (Jongens et al., 1992, Jongens et al., 1994, Robertson et al., 1999, Cinalli and Lehmann, 2013). In the absence of Gcl activity, there is a severe reduction in the total number of PGCs, i.e., the *germ cell-less* phenotype (Jongens et al., 1992). Moreover, the *gcl* PGCs inappropriately express genes that are normally only transcribed in the soma (Leatherman et al., 2002). Previous studies pointed to a role for Gcl at two steps in PGC development. The first is in the initial formation of PBs, while the second is in the cellularization of the PBs to form PGCs. The later activity requires Gcl protein localization to the nucleus and nuclear envelope, while the former does not (Robertson et al., 1999). Nonetheless, molecular mechanisms underlying Gcl function remain little understood. Critically, mutations in human Gcl (HGCL/GMCL1) are also associated with sterility (Kleiman et al., 2003). Thus, elucidating how Gcl promotes germline development in *Drosophila* will provide valuable insights into this process and may contribute to our understanding of human pathology. In the studies reported here, we have focused on the mechanisms underlying the initial function of Gcl in directing the formation of PBs. We show that Gcl mediates proper germ cell formation by regulating the spatial organization of centrosomes to promote efficient germ plasm segregation and PB formation.

Results and Discussion

Gcl is required for the even distribution of germ plasm around PB nuclei

To elucidate mechanisms of Gcl function in germ cell development, we used a combination of static and live imaging to follow the processes of PB and PGC formation in syncytial embryos. Consistent with previous work, germ plasm localization to the posterior cortex is normal in *gcl* null mutant embryos preceding the onset of PB formation (Fig. 1A; Jongens et al., 1992, Robertson et al., 1999). We next asked whether Gcl functions in the release of the germ plasm from the posterior cortex or in its distribution during PB formation.

Live time-lapse imaging of *nos*, labeled in vivo with GFP (*nos**GFP) using the transgenic MS2/MCP tagging system (Forrest and Gavis, 2003), shows normal dynamics of germ

Author Manuscript Author Manuscript Author Manuscript Author Manuscript

plasm release and the expected symmetrically bilateral accumulation around PB nuclei in wild-type (WT) embryos (Fig. 1B and Video 1). Similar to controls, germ plasm release occurs normally in *gcl* mutant embryos as evidenced by nucleus-directed runs of *nos**GFP particles and formation of discrete concentrations of *nos* adjacent to PB nuclei (Fig. 1B and Video 2). In contrast, the distribution of germ plasm around the PB nuclei is abnormal in *gcl* mutants. Two distinct phenotypes are observed. One defect is the asymmetric distribution of *nos**GFP typically biased toward the posterior surface of PB nuclei (Fig. 1B). The same asymmetric distribution is also observed for endogenous Vas in fixed *gcl* embryos (Fig. 1C). A second defect is the reduced amounts of germ plasm that accumulate around the PB nuclei in *gcl* mutants as compared to WT (Fig. 1D and 1E, Video 3). Quantification confirms that the accumulation of germ plasm around PB nuclei is disrupted in many more *gcl* mutants (N=23/41 embryos; 56%) than WT (N=3/42 embryos; 7%). These results reveal a previously unappreciated role for Gcl at a very early step in PGC development just after the point of germ plasm release. The failure to properly distribute germ plasm during PB formation means that even if the PBs manage to cellularize, they might not inherit the critical threshold of germ plasm needed to adopt the germline fate (Ewen-Campen et al., 2010). Furthermore, the aberrant germ plasm distribution likely also contributes to the reduced formation of PBs and PGCs in *gcl* mutants (Jongens et al., 1992).

MT organization is disrupted in *gcl* mutant embryos

Centrosome-nucleated astral MTs are required for the release of germ plasm from the posterior cortex and subsequent accumulation around PB nuclei to ensure that germline determinants are properly distributed to newly formed PGCs (Raff and Glover, 1989, Lerit and Gavis, 2011). Thus, one mechanism that could explain the aberrant distribution of germ plasm around *gcl* mutant PB nuclei would be an abnormal organization of astral MTs. To test this prediction, we visualized MTs throughout the cell cycle in live embryos expressing αTubulin-GFP (αTub-GFP).

Live imaging of WT embryos reveals a stereotypical pattern of MT dynamics in developing PBs. In all WT embryos analyzed (N=12), complete separation of the duplicated MT-organizing centers (MTOCs) occurs rapidly. Upon mitotic exit, the two MTOCs are initially tightly juxtaposed and extend elaborate astral MT arrays that are directed away from each other (Fig. 2A, 0:00). The initial protrusion of the PB commences when the MTOCs begin to separate (Fig. 2A, 1:00). As the MTOCs move farther apart, the PB broadens and protrudes farther from the surface of the embryo (Fig. 2A, 2:00). The PB is almost fully formed once the MTOCs move opposite each other to distal sides of the PB nucleus (Fig. 2A, 3:00). The close coordination of MTOC separation with the initial protrusion and subsequent growth of the PB suggests that centrosome position instructs the actomyosin-dependent process of PB formation (Raff and Glover, 1989).

By contrast, *gcl* mutants show irregularities in MT organization during PB formation. One of the most striking defects is that MTOC separation following mitotic exit is delayed (Fig. 2A–C). Over 40% of *gcl* mutant embryos (N=4/9) show protracted MTOC separation (>3 min to fully separate; Fig. 2C). Whereas WT MTOCs move away from each other and initiate PB formation within 1 minute following mitotic exit, the MTOCs in *gcl* mutants

Author Manuscript Author Manuscript Author Manuscript Author Manuscript

remain closely juxtaposed (Fig. 2B, 1:00). Likewise, PB formation is also delayed in *gcl* mutants. By the time WT MTOCs complete their separation and the PB has enlarged substantially, *gcl* mutant MTOCs just begin to separate and initiate PB formation (cf. Fig. 2A and B, 2:00). One minute later, PB formation is nearly complete in WT, while there is only a shallow PB in the *gcl* mutant (Fig. 2A and B, 3:00). Delays in MTOC separation on the order of 1 or 2 min are not trivial considering early embryos divide about every 10 min (Foe and Alberts, 1983). The predicted result from such delays is non-uniform association of germ plasm with PB nuclei and an overall reduction in the number of PGCs that form. Indeed, live imaging confirms that *gcl* buds often retract instead of cellularizing (N=4/10 *gcl* mutant embryos).

The close correlation between MTOC separation and PB growth argues that simple proximity of the MTOC to the cortex may not be sufficient to mediate PB formation. Instead, our data suggest that mechanical forces (or biochemical cues) transduced by the astral MTs associated with the separating MTOCs stimulate PB growth. That PB growth is impaired even after the initiation of MTOC separation in *gcl* mutants (Fig. 2B, 3:00) raises the possibility that the actin rearrangements associated with PB growth are restricted to a confined time window or perhaps responsive to a short-lived instructive signal.

Gcl promotes centrosome segregation

Centrosomes are MTOCs comprising an inner pair of centrioles surrounded by a matrix of many proteins, collectively called pericentriolar material, or PCM (Rothwell and Sullivan, 2000). A plausible hypothesis is that the aberrant organization of MTs in *gcl* mutants might be due to defects in centrosome assembly, duplication, or separation. To test these possibilities, we first examined centrosome assembly by visualizing the core centriole component Asterless (Asl; Varmark et al., 2007), as well as two key PCM proteins: Centrosomin (Cnn; Li and Kaufman, 1996) and γTubulin (γTub; Sunkel et al., 1995). The localization and overall morphology of Asl, Cnn, and γTub appears normal in both somatic and germline-fated cells in *gcl* mutants (Fig. S1A, Fig. 2, and Fig. 3). Therefore, we next examined centrosome duplication and separation in live embryos expressing Asl-YFP. For these studies, we focused on centrosome dynamics at posterior nuclei during NCs 9–10, which corresponds to the onset of germ plasm release and PB formation (Foe and Alberts, 1983).

Normally, centrosome duplication is followed by their separation to opposite sides of the nucleus (Sullivan and Theurkauf, 1995). As expected, centrosomes duplicate and segregate synchronously in WT. Relative to mitotic onset (Fig. 2D, prophase I, 0:00), the duplicated WT centrosomes begin to separate early in interphase (Fig. 2D, 10:00) and reach maximal separation by prophase II (Fig. 2D, 15:00) in phase with neighboring centrosome pairs. In *gcl* embryos, while centrosomes at posterior nuclei duplicate at approximately the same time as WT, they do not initiate centrosome separation in phase with their neighbors. As a result, centrosomes are unevenly positioned along the posterior cortex in some *gcl* mutant embryos (Fig. 2E, 15:00, circles). The variable degree of centrosome separation defects in *gcl* embryos implies that centrosome behavior is likely regulated locally at each PB nucleus. Supporting the idea that Gcl functions locally at the posterior pole in regulating the timing of

Author Manuscript Author Manuscript Author Manuscript Author Manuscript

centrosome separation at PB nuclei, centrosome separation occurs normally in the soma of *gcl* mutant embryos (Fig. S1A).

To begin to delineate how Gcl functions in centrosome segregation, we tracked centrosome dynamics from our live imaging experiments. WT embryos require about 150s after centrosome duplication to fully segregate their centrosomes to distal poles of a PB nucleus (Fig. 2F, see Methods). In contrast, *gcl* mutant embryos require over 200s, which is nearly 25% slower than controls. During prophase, when the majority of centrosomes have fully separated, nearest-neighbor analysis confirms *gcl* mutants are more likely to display unevenly distributed clusters of centrosomes (Fig. S1B and S1B′, see Methods), indicating some centrosomes are closer together than others. Taken together, our findings demonstrate that Gcl functions both in timing when the duplicated centrosomes initiate separation and in setting the pace of separation.

To quantify defects in centrosome separation in *gcl* mutants versus WT, we measured the distance between centrosomes at NC 10 PBs that are in prophase (pH3 positive, see Methods) using either Cnn or Asl to mark centrosome position (Fig. 2G and S2A). In *gcl* mutants, quantification confirms that over 70% of NC 10 PBs show defects in centrosome separation (N=36/49 mutant PBs), resulting in ~30% reduction in centrosome distance relative to WT (Fig. 2H). Our analysis of centrosome separation defects correlates well with early reports showing 70% of *gcl* null embryos fail to form pole cells/PGCs (Robertson et al., 1999).

Delays in centrosome segregation in *gcl* mutants could slow cell cycle progression of the PB nuclei. Alternatively, delays in centrosome segregation may arise in *gcl* mutants due to aberrant cell cycle progression. To explore these possibilities, we examined the cell cycle progression of PB nuclei in WT and *gcl* mutant embryos with either normal or defective centrosome dynamics. Mitotic progression, as indicated by pH3 positive nuclei, appears unaltered irrespective of centrosome separation defects in *gcl* mutant embryos (Fig. 2G, arrows, and Fig. S1C). Furthermore, live imaging of αTub-GFP or Cnn-GFP to measure the timing of prophase onset or nuclear envelope breakdown reveals the duration of the cell cycle is not significantly altered for the posterior nuclei in WT versus *gcl* embryos (Fig. S1D). These data support a more direct role for Gcl in regulating centrosome separation.

An extreme consequence of failing to properly separate centrosomes is the formation of PGCs with supernumerary centrosomes. We found a small number of *gcl* mutant PGCs contain extra centrosomes (N=4/172 cells from 28 embryos; Fig. S2A), an event never observed in controls (N= 0/161 cells from 27 embryos). Although this result is not statistically significant (p=0.0543 by chi-square test), it suggests that *gcl* embryos may be susceptible to deleterious multipolar spindles. Indeed, live imaging reveals multipolar spindles in a subset of *gcl* embryos (N=2/9; Fig. S2B), a result never observed in WT (N>15 embryos). These results further support a role for Gcl in regulating centrosome segregation dynamics.

What accounts for the incomplete penetrance of centrosome defects observed in *gcl* mutants? For one, Gcl may function to tune the rate of centrosome separation by grading the

Author Manuscript Author Manuscript Author Manuscript Author Manuscript

activity of a molecular motor. Alternatively, Gcl alone may not be sufficient to regulate centrosome dynamics. Rather, loss of Gcl may be compensated by unidentified, partially redundant factors. Nonetheless, our identification of a role for Gcl in regulating centrosome separation demonstrates that PGC determinants functionally regulate centrosomes and the resulting distribution of astral MTs. While prior studies indicated centrosomes/astral MTs are needed to orchestrate PGC formation, our work implicates factors within the germ plasm reciprocally influencing centrosome behavior.

Defects in centrosome separation result in impaired germ plasm distribution

Our findings raise the possibility that the unequal distribution of *nos* and Vas in *gcl* mutant PBs (Fig. 1) is a consequence of the defects in centrosome separation and astral MT organization. To directly assess the relationship between germ plasm distribution and centrosome position, we examined the enrichment of germ plasm relative to PB centrosomes and MTs in WT and *gcl* mutant embryos. For these studies, we focused on the processes of PB formation and PGC cellularization – events where Gcl was previously implicated (Jongens et al., 1992).

Immunostaining for Cnn to label centrosomes, αTub to display MTs, and Vas to mark germ plasm demonstrates that germ plasm accumulates preferentially in areas of MT-enrichment (Fig. 3). Imaging nascent PBs during NC 10 reveals much of the Vas protein decorates astral MTs that extend from each well-separated centrosome (Fig. 3A; inset). In *gcl* mutants, Vas also preferentially accumulates along the astral MTs that emanate from centrosomes (Fig. 3B and inset). However, since the duplicated centrosomes are still tightly juxtaposed and there is no PB, much of the Vas remains asymmetrically concentrated in smaller domains. Our data thus suggest that the failure to effectively separate centrosomes in *gcl* mutant embryos may underlie the inability to both form PBs and properly distribute germ plasm around PB nuclei.

Later in development, PGC proliferation is marked by the symmetric segregation of Vas into both daughter cells in association with the astral MTs (Fig. 3C, inset; Lerit and Gavis, 2011). Thus, germ plasm is normally restricted to the PGCs in WT embryos. However, because many PBs regress and PGCs fail to form in *gcl* mutant embryos, Vas remains unevenly distributed among centrosomes associated with nuclei situated along the posterior cortex (Fig. 3D and Fig. S3).

Centrosome separation is required for germ plasm distribution and PB formation

Our previous work examining various centrosome mutants revealed a number of phenotypes similar to loss of *gcl*, including abnormal germ plasm distribution and PGC loss (see Fig. 5 in Lerit and Gavis, 2011). Further similarity is also evident in the initial steps of PB formation by the growth of shallow and abnormally shaped PBs in *cnn* null embryos (Fig. 4A). These data highlight the critical role of centrosomes and their associated astral MTs in promoting PGC development.

Our characterization of Gcl function points to a more precise mechanism regulating centrosome separation. To test our model that Gcl functions primarily through regulating centrosome dynamics, we asked whether defects in centrosome separation are sufficient to

Author Manuscript Author Manuscript Author Manuscript Author Manuscript

disrupt PB formation. For these studies, we expressed a mutant form of the Cnn protein, CnnΔCM1, which exerts dominant effects to impair centrosome separation (Zhang and Megraw, 2007). Normally, WT embryos form broad, convex PBs. In contrast, nearly 40% of embryos expressing CnnΔCM1 produce small and narrow PBs (N=11/29 CnnΔCM1 embryos cf. N=3/32 WT embryos; Fig. 4B), supporting a role for centrosome separation in driving PB protrusion.

To independently verify a role for centrosome separation in PGC development without altering the activity of Cnn, we examined germ plasm distribution and PB growth via RNAi-mediated knock-down of the kinesin motor Klp61F/Eg5, which is critical for normal centrosome separation dynamics (Heck et al., 1993). Due to the range of mitotic defects observed in $Eg5^{RNAi}$ embryos, we limited our analysis to those embryos where nuclei had migrated to the posterior pole. Importantly, those embryos displaying impaired PB centrosome separation upon depletion of *Eg5* also show irregular distributions of germ plasm (Fig. 4C) that resemble the uneven patterns noted in *gcl* mutant embryos (Figs. 1B and 1C). Asymmetric accumulation of germ plasm is observed in ~40% of $Eg5^{RNAi}$ embryos (N=8/21 RNAi embryos; cf. N=1/21, 4.7% WT embryos). In addition, ~50% of the *Eg5*-depleted embryos examined display misshaped PBs (Fig. 4C; N=40 embryos) similar to CnnΔCM1 embryos (Fig. 4B). We conclude that proper centrosome separation is necessary to promote normal germ plasm segregation and robust PB growth.

Centrosomes contribute to PGC cellularization

Following the induction of PB budding, *gcl* has a later function in the cellularization of the PGCs (Jongens, et al. 1992). PGC cellularization requires the concerted action of many proteins that regulate the organization of the actin cytoskeleton, including Anillin, to mediate closure of the PB furrow (Field et al., 2005). Recent studies suggest that *gcl* could play a role in controlling the reorganization of the actin cytoskeleton during PB furrow closure via Anillin (Cinalli and Lehmann, 2013) and/or Steppke (Step), a recently identified antagonist of Rho1 (Lee et al., 2015). Loss of Step activity results in precocious cellularization in the soma, while overexpressing Step blocks PGC formation by a mechanism that involves antagonizing Gcl activity (Lee et al., 2015).

It is currently unknown whether Gcl might regulate actin directly or indirectly to mediate PB furrow closure. In the soma of the syncytial embryo, there is a well-established connection between centrosome position and actin organization. During interphase, apical centrosome pairs organize actin into caps, while centrosome separation shifts actin into basal furrows (Rothwell and Sullivan, 2000). Further mutant and pharmacological studies demonstrate a functional link between centrosome position and actin organization in the syncytial embryo (Cao et al., 2010). Moreover, a link between actin and centrosome position is well conserved, as actin-binding proteins have been implicated in regulating centrosome positioning in diverse cell types harboring supernumerary centrosomes (Kwon et al., 2008, Sabino et al., 2015). Likewise, during PGC development, colchicine injection immediately after PB formation produces stable PBs that fail to cellularize (Raff and Glover, 1989; DAL and ERG unpublished results). However, a recent report suggests that MTs are dispensable for PB furrow closure (Cinalli and Lehmann, 2013). To revisit the requirement for MTs in

Author Manuscript Author Manuscript Author Manuscript Author Manuscript

PGC celluarization and to investigate whether Gcl function in PB furrow closure may represent an extension of its centrosome-dependent activities during PB formation, we genetically manipulated centrosome integrity and/or position.

To assess a role for centrosomes in PGC cellularization, we first examined PB furrow closure in the few mature PBs that form in *cnn* embryos. In WT embryos, PB furrows are readily observed by immunostaining for Anillin (N=10/10 embryos; 100%; Fig. 4A). In contrast, we found nearly half of the mature PBs in *cnn* embryos lack a clear Anillin ring (N=11/27 embryos; 40%; Fig. 4A). Aberrant Anillin organization was also observed in CnnΔCM1 embryos, which organize an irregular and punctate distribution of Anillin at the PB furrow (Fig. 4B and inset). Moreover, quantitation of PGCs in NC 13–14 embryos indicates normal centrosome separation is required for PGC cellularization (Fig. 4D). Embryos expressing CnnΔCM1 (N=6.8±3.6 PGCs, 13 embryos; $p<0.0001$ by Student's t-test) or $Eg5^{RNAi}$ (N=7.0±4.7 PGCs, 25 embryos; $p<0.0001$) reveal a significant reduction in PGCs as compared to WT (N=19.9±5.3 PGCs, 20 embryos). Collectively, these studies argue that centrosome position instructs PB growth and PGC cellularization and support a model in which Gcl regulates PB and PGC development by orchestrating centrosome behavior (Fig. S4).

To date, the only other factors known to disrupt germ plasm distribution at nascent PBs are cytoskeletal elements involved in germ plasm transport (Lerit and Gavis, 2011). Identification of Gcl as a localized regulator of centrosome behavior hints that other germ plasm factors may also contribute to this process. Precisely how Gcl coordinates centrosome behavior is an exciting area of future research. We propose that throughout PGC development, Gcl serves as a mechanistic bridge between centrosomes and the actin cytoskeleton. Previous work shows that Gcl ectopically localized to the nucleus or cytoplasm largely rescues PB budding in *gcl* null embryos (Robertson et al., 1999). While cytoplasmic Gcl may be accessible to centrosomes, the finding that nucleoplasmic Gcl rescues PB growth raises the possibility that Gcl regulates centrosome dynamics indirectly. While future work is required to tease out the relationship between centrosomes, Gcl, and actin regulators, our studies provide insights into how the regulation of centrosome position by Gcl contributes to the efficient segregation of the germline determinants, promotes PB formation, and, ultimately, instructs the precocious cellularization of the PGCs.

Materials and Methods

Fly Stocks

The following mutant and transgenic lines were used: $y^1 w^{1118}$ was used as the WT control unless otherwise noted; Δ*gcl* is a null allele (Robertson, et al. 1999); $nos(MS2)_{18}$ (Brechbiel and Gavis, 2008); *hsp83-MCP-GFP* (Forrest and Gavis, 2003); *Ubi-Asl-YFP* (Rebollo et al., 2007); a recombinant line of *maternal Tubulin-GAL4, UASp-GFP-α Tubulin* (Lucas and Raff, 2007); *UASp-CnnΔCM1* (Zhang and Megraw, 2007) and $UASp\text{-}Eg5^{RNAi}$ (VDRC KK line: 109280) were driven by *maternal 67C Tubulin-GAL4* (Lee et al., 2001). Mutant and transgenic embryos derive from mutant or transgenic females mated to sibling or $y^1 w^{1118}$ males.

Author Manuscript Author Manuscript Author Manuscript Author Manuscript

Image Analysis

The line tool in ImageJ was used to measure the distance between centrosomes within a given centrosome pair in NC 10 embryos during prophase, as determined by the presence of round, DAPI-condensed nuclei and/or anti-pH3 signal. The time elapsed during centrosome separation is defined as the time from the splitting of a centrosome pair until the time when those centrosomes reach maximal separation prior to anaphase onset. For centrosome position analysis, binary masks corresponding to images of centrosomes from prophase-stage embryos in NCs 10 or 11 were extracted from maximum fluorescence intensity projections and subjected to nearest-neighbor analysis using the Particle Distribution (2D) function in the Biovoxxel Toolbox Plug-in (Jan Brocher) using FIJI software. Distances between objects (here, centrosomes at the posterior pole) are measured with respect to a theoretical nearest-neighbor distance that represents a normal randomized distribution. Self-avoiding centrosomes are spaced farther apart than the expected theoretical distance, while clustered centrosomes are spaced closer together than the expected theoretical distance.

Statistical Methods

Data were plotted and statistical analysis was performed using Microsoft Excel and GraphPad Prism software. To calculate significance, distribution normality was first confirmed with a D'Agnostino and Pearson normality test. Data were then analyzed by Student's two-tailed *t*-test or the Wilcoxon rank-sum test unless noted and are displayed as mean ± standard deviations (SD).

Supplementary Material

Refer to Web version on PubMed Central for supplementary material.

Acknowledgments

For reagents, we acknowledge the Bloomington Stock Center, Vienna *Drosophila* Resource Center, and Drs. Ruth Lehmann, Paul Lasko, Tim Megraw, Christine Field, and Greg Rogers. We thank Dr. Gary Laevsky and the Princeton Molecular Biology Confocal Microscopy Facility, a Nikon Center of Excellence. Gordon Grey and Cliff Sonnenbrot provided fly media. This work was supported by NIH grants R01GM110015 to PS and GD, R01GM067758 to ERG, 1ZIAHL006126 to NMR, and 1K22HK126922-01A1 to DAL. PS is a recipient of a Ministry of Education and Science of the Russian Federation grant (14.B25.31.0022).

References

BRECHBIEL JL, GAVIS ER. Spatial regulation of *nanos* is required for its function in dendrite morphogenesis. Curr Biol. 2008; 18:745–750. [PubMed: 18472422]

CAO J, et al. Cortical actin dynamics facilitate early-stage centrosome separation. Curr Biol. 2010; 20:770–776. [PubMed: 20409712]

CINALLI RM, LEHMANN R. A spindle-independent cleavage pathway controls germ cell formation in *Drosophila*. Nat Cell Biol. 2013; 15:839–845. [PubMed: 23728423]

EWEN-CAMPEN B, SCHWAGER EE, EXTAVOUR CG. The molecular machinery of germ line specification. Mol Reprod Dev. 2010; 77:3–18. [PubMed: 19790240]

FIELD CM, COUGHLIN M, DOBERSTEIN S, MARTY T, SULLIVAN W. Characterization of *anillin* mutants reveals essential roles in septin localization and plasma membrane integrity. Development. 2005; 132:2849–2860. [PubMed: 15930114]

Author Manuscript Author Manuscript Author Manuscript Author Manuscript

FOE VE, ALBERTS BM. Studies of nuclear and cytoplasmic behaviour during the five mitotic cycles that precede gastrulation in *Drosophila* embryogenesis. J Cell Sci. 1983; 61:31–70. [PubMed: 6411748]

FORREST KM, GAVIS ER. Live imaging of endogenous RNA reveals a diffusion and entrapment mechanism for *nanos* mRNA localization in *Drosophila*. Curr Biol. 2003; 13:1159–1168. [PubMed: 12867026]

HECK MM, PEREIRA A, PESAVENTO P, YANNONI Y, SPRADLING AC, GOLDSTEIN LS. The kinesin-like protein KLP61F is essential for mitosis in *Drosophila*. J Cell Biol. 1993; 123:665–679. [PubMed: 8227131]

JONGENS TA, ACKERMAN LD, SWEDLOW JR, JAN LY, JAN YN. Germ cell-less encodes a cell type-specific nuclear pore-associated protein and functions early in the germ-cell specification pathway of *Drosophila*. Genes Dev. 1994; 8:2123–2136. [PubMed: 7958883]

JONGENS TA, HAY B, JAN LY, JAN YN. The *germ cell-less* gene product: a posteriorly localized component necessary for germ cell development in *Drosophila*. Cell. 1992; 70:569–584. [PubMed: 1380406]

KLEIMAN SE, YOGEV L, GAL-YAM EN, HAUSER R, GAMZU R, BOTCHAN A, PAZ G, YAVETZ H, MAYMON BB, SCHREIBER L, BARZILAI S, AMARIGLIO N, RECHAVI G, SIMON AJ. Reduced human germ cell-less (HGCL) expression in azoospermic men with severe germinal cell impairment. J Androl. 2003; 24:670–675. [PubMed: 12954656]

KWON M, GODINHO SA, CHANDHOK NS, GANEM NJ, AZIOUNE A, THERY M, PELLMAN D. Mechanisms to suppress multipolar divisions in cancer cells with extra centrosomes. Genes Dev. 2008; 22:2189–2203. [PubMed: 18662975]

LASKO PF, ASHBURNER M. Posterior localization of vasa protein correlates with, but is not sufficient for, pole cell development. Genes Dev. 1990; 4:905–921. [PubMed: 2384213]

LEATHERMAN JL, LEVIN L, BOERO J, JONGENS TA. *germ cell-less* acts to repress transcription during the establishment of the *Drosophila* germ cell lineage. Curr Biol. 2002; 12:1681–1685. [PubMed: 12361572]

LEE DM, WILK R, HU J, KRAUSE HM, HARRIS TJ. Germ Cell Segregation from the *Drosophila* Soma Is Controlled by an Inhibitory Threshold Set by the Arf-GEF Steppke. Genetics. 2015; 200:863–872. [PubMed: 25971667]

LEE MJ, GERGELY F, JEFFERS K, PEAK-CHEW SY, RAFF JW. Msps/XMAP215 interacts with the centrosomal protein D-TACC to regulate microtubule behaviour. Nat Cell Biol. 2001; 3:643–649. [PubMed: 11433296]

LERIT DA, GAVIS ER. Transport of germ plasm on astral microtubules directs germ cell development in *Drosophila*. Curr Biol. 2011; 21:439–448. [PubMed: 21376599]

LI K, KAUFMAN TC. The homeotic target gene *centrosomin* encodes an essential centrosomal component. Cell. 1996; 85:585–596. [PubMed: 8653793]

LUCAS EP, RAFF JW. Maintaining the proper connection between the centrioles and the pericentriolar matrix requires *Drosophila centrosomin*. J Cell Biol. 2007; 178:725–732. [PubMed: 17709428]

MAHOWALD AP. Assembly of the *Drosophila* germ plasm. Int Rev Cytol. 2001; 203:187–213. [PubMed: 11131516]

RAFF JW, GLOVER DM. Centrosomes, and not nuclei, initiate pole cell formation in *Drosophila* embryos. Cell. 1989; 57:611–619. [PubMed: 2497990]

RAFF JW, WHITFIELD WG, GLOVER DM. Two distinct mechanisms localise *cyclin B* transcripts in syncytial *Drosophila* embryos. Development. 1990; 110:1249–1261. [PubMed: 2151612]

REBOLLO E, SAMPAIO P, JANUSCHKE J, LLAMAZARES S, VARMARK H, GONZALEZ C. Functionally unequal centrosomes drive spindle orientation in asymmetrically dividing *Drosophila* neural stem cells. Dev Cell. 2007; 12:467–474. [PubMed: 17336911]

ROBERTSON SE, DOCKENDORFF TC, LEATHERMAN JL, FAULKNER DL, JONGENS TA. *germ cell-less* is required only during the establishment of the germ cell lineage of *Drosophila* and has activities which are dependent and independent of its localization to the nuclear envelope. Dev Biol. 1999; 215:288–297. [PubMed: 10545238]

Author Manuscript Author Manuscript Author Manuscript Author Manuscript

ROTHWELL WF, SULLIVAN W. The centrosome in early *Drosophila* embryogenesis. Curr Top Dev Biol. 2000; 49:409–447. [PubMed: 11005030]

SABINO D, GOGENDEAU D, GAMBAROTTO D, NANO M, PENNETIER C, DINGLI F, ARRAS G, LOEW D, BASTO R. Moesin is a major regulator of centrosome behavior in epithelial cells with extra centrosomes. Curr Biol. 2015; 25:879–889. [PubMed: 25772448]

SMITH JL, WILSON JE, MACDONALD PM. Overexpression of oskar directs ectopic activation of nanos and presumptive pole cell formation in *Drosophila* embryos. Cell. 1992; 70:849–859. [PubMed: 1516136]

SULLIVAN W, THEURKAUF WE. The cytoskeleton and morphogenesis of the early *Drosophila* embryo. Curr Opin Cell Biol. 1995; 7:18–22. [PubMed: 7755985]

SUNKEL CE, GOMES R, SAMPAIO P, PERDIGAO J, GONZALEZ C. Gamma-tubulin is required for the structure and function of the microtubule organizing centre in *Drosophila* neuroblasts. The EMBO journal. 1995; 14:28–36. [PubMed: 7828594]

VARMARK H, LLAMAZARES S, REBOLLO E, LANGE B, REINA J, SCHWARZ H, GONZALEZ C. Asterless is a centriolar protein required for centrosome function and embryo development in *Drosophila*. Curr Biol. 2007; 17:1735–45. [PubMed: 17935995]

WARN RM, SMITH L, WARN A. Three distinct distributions of F-actin occur during the divisions of polar surface caps to produce pole cells in *Drosophila* embryos. J Cell Biol. 1985; 100:1010–1015. [PubMed: 3980576]

ZHANG J, MEGRAW TL. Proper recruitment of gamma-tubulin and D-TACC/Msps to embryonic Drosophila centrosomes requires *Centrosomin* Motif 1. Mol Biol Cell. 2007; 18:4037–4049. [PubMed: 17671162]

Author Manuscript Author Manuscript Author Manuscript Author Manuscript

Highlights

- Germ cell-less (Gcl) promotes germline fate determinant segregation into germ cells
- Gcl mediates efficient centrosome separation dynamics
- Centrosome positioning instructs germ cell precocious cellularization

Author Manuscript Author Manuscript Author Manuscript Author Manuscript

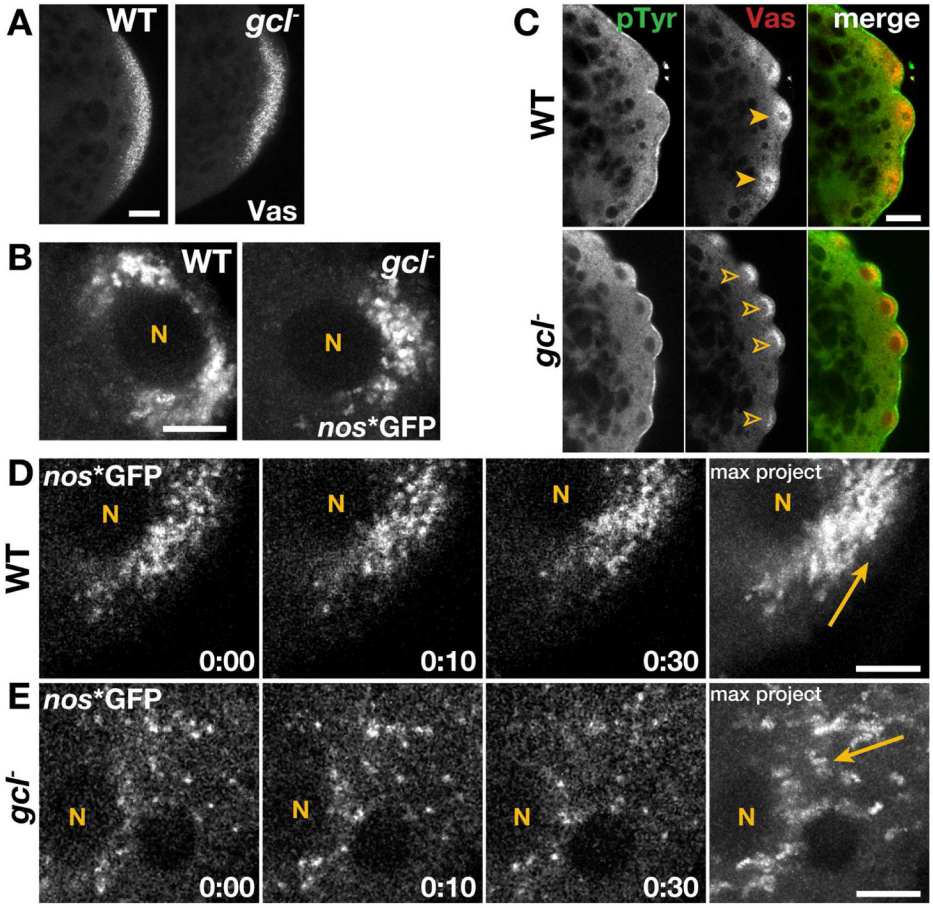

Figure 1. Germ plasm distribution is aberrant in *gcl* embryos

In all images, posterior is to the right. (A) Immunofluorescence for Vas in 0–1 hr WT and *gcl* embryos. (B) Maximum intensity projections show 8.3s of elapsed time from live 1–2 hr embryos expressing *nos**GFP. (C) 1–2 hr embryos stained for the indicated proteins; closed arrowheads, symmetric Vas; open arrowheads, uneven/reduced Vas. (D and E) Time-lapse imaging of *nos**GFP in live 1–2 hr embryos. Time is shown min:s; "N", PB nuclei; arrows mark trajectory of *nos**GFP. Bars: (A and C) 20 μm; (B, D, and E) 5 μm.

Author Manuscript Author Manuscript Author Manuscript Author Manuscript

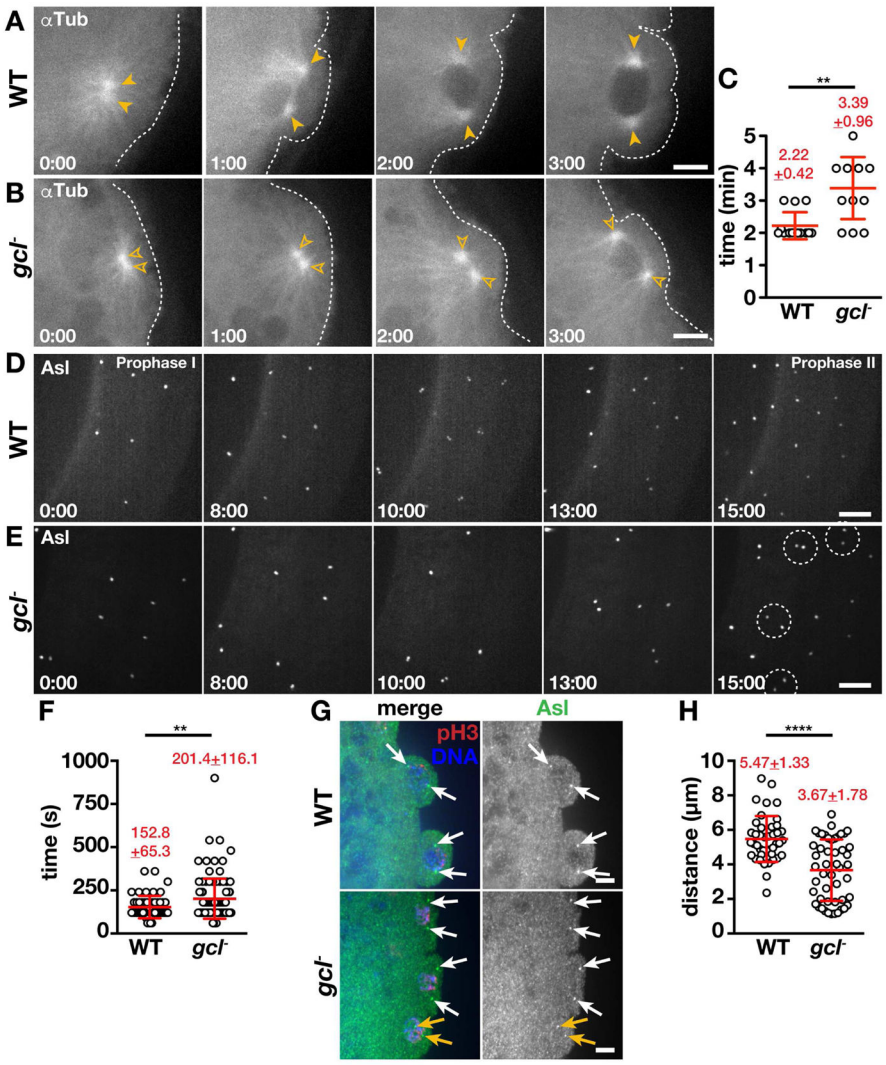

Figure 2. Gcl is required for MT organization

(A and B) Time-lapse imaging of αTub-GFP in 1–2 hr embryos; arrowheads, MTOCs; dashed lines, cortex. (C) Quantification of MTOC separation timing. Each data point indicates the time it takes for a pair of MTOCs to separate in WT (N=14 events in 12 embryos) and *gcl* (N=13 events in 9 embryos). (D and E) Maximum intensity projections from live imaging of Asl-YFP. Time is relative to prophase onset (0:00) and shown min:s. Centrosome separation delays are highlighted (dashed circles). (F) Quantification of centrosome segregation timing in WT (N=53 events in 9 embryos) and *gcl* (N=112 events in 17 embryos). (G) Prophase-stage NC 10 embryos stained for the indicated proteins; arrows mark complete (white) or incomplete (orange) centrosome separation. (H) Quantification of centrosome distance during prophase NC 10 (N=42 pairs from 10 WT embryos and N=49 pairs from 9 *gcl* embryos). Statistical significance was determined using a two-tailed Mann-Whitney test, **** $p<0.0001$, ** $p<0.01$. Bars: 5 μm. See also Figures S1 and S2.

Author Manuscript Author Manuscript Author Manuscript Author Manuscript

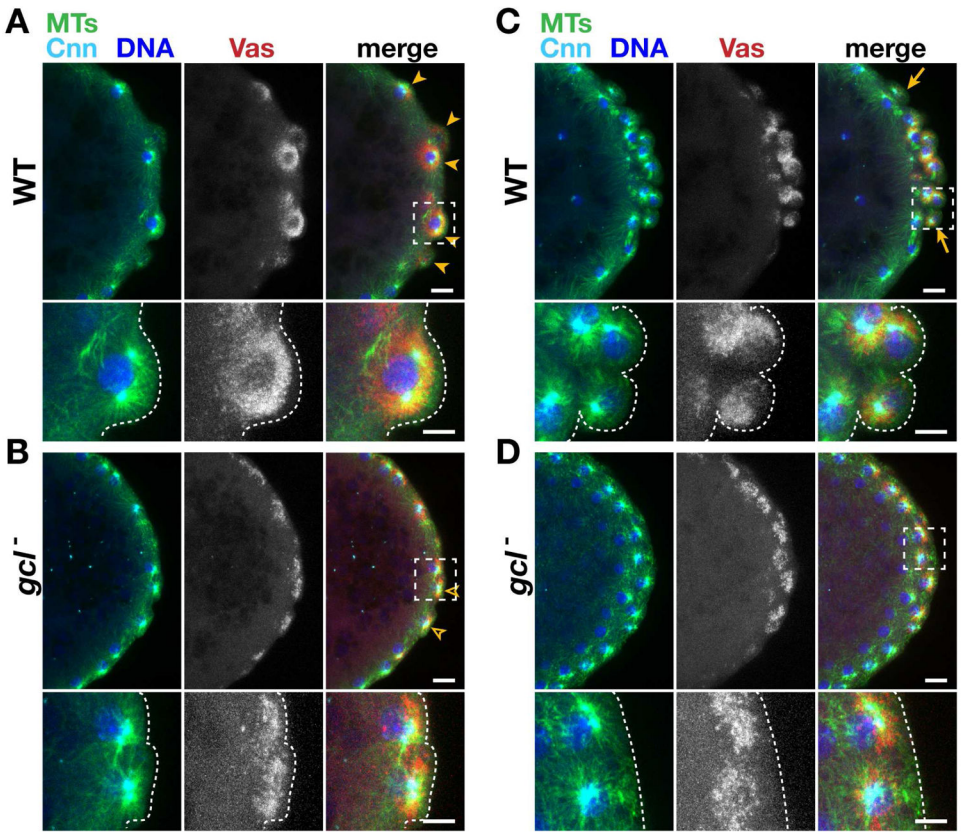

Figure 3. Centrosome segregation instructs germ plasm distribution

Immunofluorescence for the indicated proteins during (A and B) PB formation and (C and D) PGC formation. Boxes show inset enlarged below; dashed lines mark the posterior cortex. Arrowheads show PBs, and arrows delineate the PGC cluster. Bars: 10 μm; insets 5 μm. See also Figure S3.

Author Manuscript Author Manuscript Author Manuscript Author Manuscript

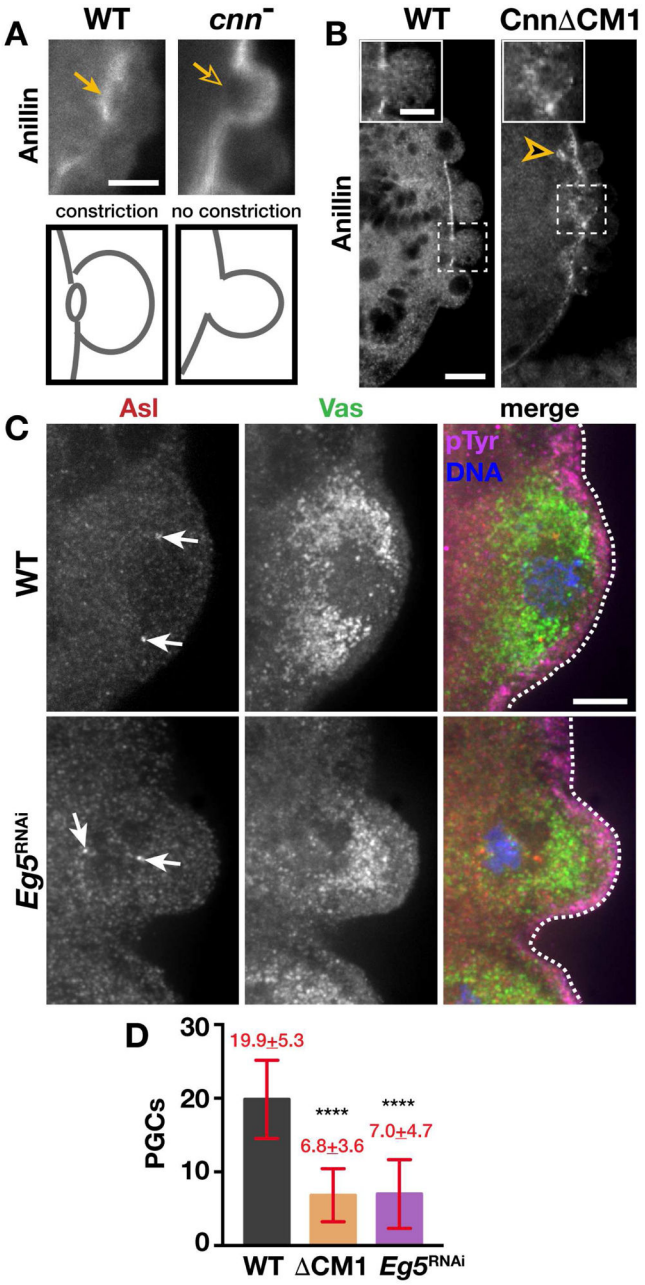

Figure 4. Functional centrosomes promote PGC formation

(A and B) Immunofluorescence for Anillin in 1–2 hr embryos. (A) Arrows note the presence (closed) or absence (open) of the Anillin ring (PB furrow). (B) Insets show Anillin distribution; arrowhead, Anillin puncta. (C) Immunofluorescence for the indicated proteins in NC 10 embryos; arrows, centrosomes; dashed lines, cortex. (D) Quantification of PGCs in NC 13–14 embryos. Statistical significance was determined by Student's t-test, **** $p<0.0001$. Bars: (A and B) 10 μm; insets in (B), 5 μm; (C) 5 μm. See also Figure S4.